


Y. CHENG¹
H.L. TSAI¹,
K. SUGIOKA²
K. MIDORIKAWA²

Fabrication of 3D microoptical lenses in photosensitive glass using femtosecond laser micromachining

¹ Laser-Based Manufacturing Laboratory, Department of Mechanical & Aerospace Engineering, University of Missouri-Rolla, 1870 Miner Circle, Rolla, MO 65409, USA

² Laser Technology Laboratory, RIKEN – The Institute of Physical and Chemical Research, Hirosawa 2-1, Wako, Saitama 351-0198, Japan

Received: 9 May 2006 / Accepted: 20 July 2006
Published online: 10 August 2006 • © Springer-Verlag 2006

ABSTRACT We describe the fabrication of microoptical cylindrical and hemispherical lenses vertically embedded in a photosensitive Foturan glass by femtosecond (fs) laser three-dimensional (3D) micromachining. The process is mainly composed of four steps: (1) fs laser scanning in the photosensitive glass to form curved surfaces (spherical and/or cylindrical); (2) postannealing of the sample for modification of the exposed areas; (3) chemical etching of the sample for selective removal of the modified areas; and (4) a second postannealing for smoothening the surfaces of the tiny lenses. We examine the focusing ability of the microoptical lenses using a He-Ne laser beam, showing the great potential of using these microoptical lenses in lab-on-a-chip applications.

PACS 42.62.-b; 81.05.Kf; 82.50.Pt

1 Introduction


The concept of lab-on-a-chip has created a revolution in chemical, biological, and medical sciences [1]. A lab-on-a-chip device, which is a palm-sized chip integrated with functional components such as microfluidics, microoptics, microelectronics, and micromechanics, offers several advantages over the traditional chemical and biological analysis techniques [2]. Because of its tiny dimensions, the lab-on-a-chip allows for performing of chemical and biological analysis with ease of use, low sample and reagent consumption, low waste production, high speed of analysis, and high reproducibility due to standardization and automation. Recently, significant progress has been made in the incorporation of optical circuits into the fluidic circuits, which would eventually enable enhanced functionality of the lab-on-a-chip devices. A variety of optical structures, including opti-

cal waveguides [3], microoptical gratings [4], optical fibers [5], microoptical mirrors [6], and microoptical cylindrical lenses [7], have been used in the construction of fluidic photonic integrated devices. In this work, we demonstrate for the first time to our best knowledge, the fabrication of three-dimensional (3D) microoptical cylindrical and hemispherical lenses vertically embedded in glass using a home-integrated femtosecond (fs) laser micromachining system. We will also show that these microoptical lenses can focus laser beams into small light spots, holding promise for practical applications in life sciences.

We briefly introduce here the mechanism of fs laser micromachining of Foturan glass, because the details can be found elsewhere [8–10]. The photosensitive glass Foturan is composed of lithium aluminosilicate glass and doped with a trace amount of silver and cerium. Traditionally, microstructures on the surface of Foturan glass

can be patterned using UV lithography (290–330 nm). In this case, the cerium (Ce^{3+}) ion play the important role of photosensitizer, which releases an electron to become Ce^{4+} by exposure to UV light irradiation. Some silver ions then capture the free electrons to form silver atoms. In a subsequent heat treatment, the silver atoms first diffuse and agglomerate to form clusters at a temperature of around 500 °C; and then the crystalline phase of lithium metasilicate grows around the silver clusters as the nucleus in the amorphous glass matrix at a temperature of around 600 °C. Since this crystalline phase of lithium metasilicate has an etching rate in a dilute solution of hydrofluoric (HF) acid which is much higher than the glass matrix, it can be preferentially etched away, leaving behind the engraved pattern on the glass surface.

However, the microstructuring of Foturan glass by UV lithography is limited to the sample surface because of the resonant absorption of UV light starting at the sample surface. To overcome this issue, lasers working at non-resonant wavelengths, including nanosecond (ns) lasers at 355 nm [9] and fs lasers at 400 nm and 755 nm [8, 10, 11], were employed to fabricate 3D microstructures buried in Foturan glass without damage to the surface. Since these wavelengths are outside of the absorption band of Foturan glass, photo-modification of glass can only be initiated near the focal point where the extremely high laser intensity induces nonlinear optical effects like multiphoton absorption. It has been found that the photochemistry of fs laser modification of Foturan glass is different from the

 Fax: +1-573-341-4607, E-mail: tsai@umr.edu

established theory for UV light processing, because photo-reduction of silver with fs laser irradiation is possible even without Ce^{3+} ions [12, 13]. Deeper investigation is still required for building a thorough physical understanding for fs laser modifications of Foturan glass.

2 Experimental

The experiments were carried out at a home-integrated fs laser 3D micromachining system. The repetition rate, center wavelength and pulse width of the fs laser (Legend-F, Coherent) were 1 kHz, 800 nm and 120 fs, respectively. The maximum output power of the fs laser was approximately 1 W; however, we used a combination of a half-waveplate and a polarizer to first reduce the laser power to 20 mW, and then used several neutral density (ND) filters to further reduce the laser power to desirable values based on different experimental conditions. The attenuated laser beam was directed into objective lenses (Olympus UMPLFL10 \times , and 20 \times) with different numerical apertures (NA) and finally focused into the glass samples. For fabrication of 3D microstructures, Foturan glass samples were translated by a five-axis motion stage (Aerotech) with a resolution of 1 μ m. The Foturan glass sheets of 2 mm thickness were bought from Mikroglass Chemtech. Before being used in the experiments, the glass sheet was cut into small coupons by a diamond cutter.

In the first step of our experiment, we scanned the tightly focused fs laser beam inside the samples to form curved surfaces embedded in Foturan glass. To fabricate the microoptical cylindrical lens, we scanned a pile of parallel ring structures with the same radius from the top to the bottom of the glass. In this case, a 10 \times objective lens with NA = 0.3 was used in the processing. The vertical space between each of the two adjacent parallel rings in the glass was 15 μ m. The laser pulse energy before the objective lens was measured as 800 nJ, which was slightly below the ablation threshold as we observed in the experiment. To fabricate the microoptical hemispherical lens, we changed the radius of each ring structure at a different depth to form a spherical surface inside the glass. In this case, in order to obtain a high fabrication resolution

in the vertical direction, a 20 \times objective lens with NA = 0.45 was used in the processing. The vertical space between each of the two adjacent parallel rings in the glass was reduced to 7.5 μ m. The laser pulse energy before the objective lens was measured as 400 nJ. In both of these two experiments, the scanning speed of the rotary stage was fixed at 360 $^\circ$ /min. Lastly, to break the cylindrical and the spherical structures into two equal parts, we scanned the focused fs laser to form a vertical plane through the center of the rings which would eventually result in two equal parts after the following annealing and subsequent chemical etching of the glass coupon.

After the laser scanning process, we baked the exposed sample at 500 $^\circ$ C for 1 h and then at 605 $^\circ$ C for another 1 h in a programmable furnace (Fisher Scien-

tific). After this step, we etched the sample in a solution of 10% HF acid diluted in water in an ultrasonic bath for one hour to remove modified areas. Lastly, we baked the etched sample again at 560 $^\circ$ C for 5 h for further smoothing of the surfaces of the microlenses. This annealing temperature is slightly lower than the one (570 $^\circ$ C) used in our previous work [14], because the actual temperature in different furnaces may not be the same even at a same setting point. In the discussion (Sect. 4) of this paper, we will give a general principle to optimize the annealing temperature for different furnaces.

3 Results

First, we fabricated microoptical cylindrical lenses with a radius of 1 mm, as shown in Fig. 1. For compar-

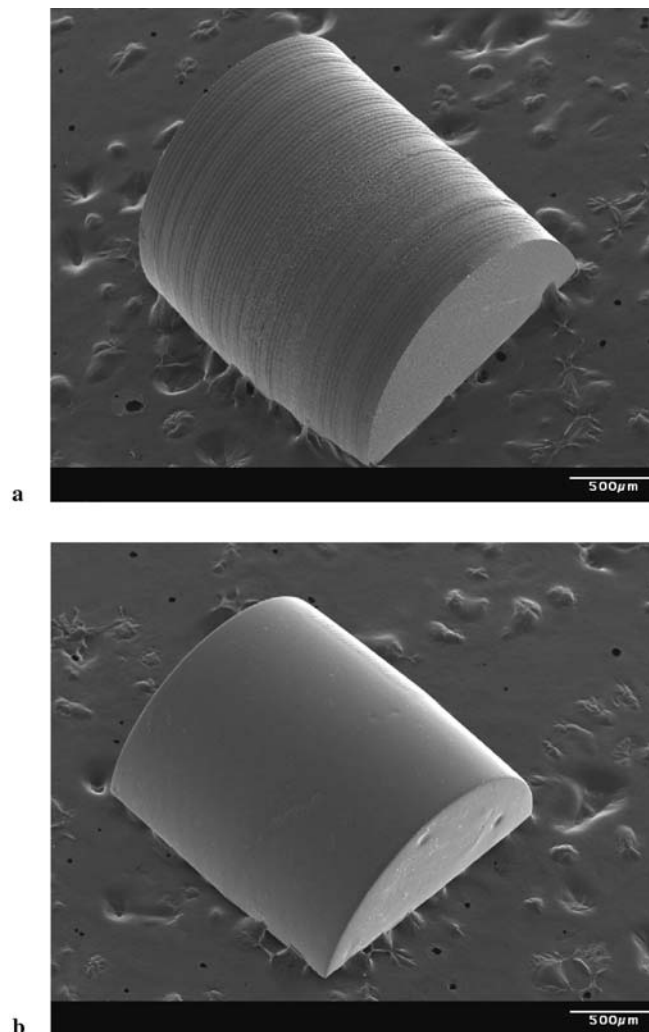


FIGURE 1 SEM images of microoptical cylindrical lenses fabricated by fs laser 3D micromachining. (a) Without a final smoothing step; (b) With a final smoothing step

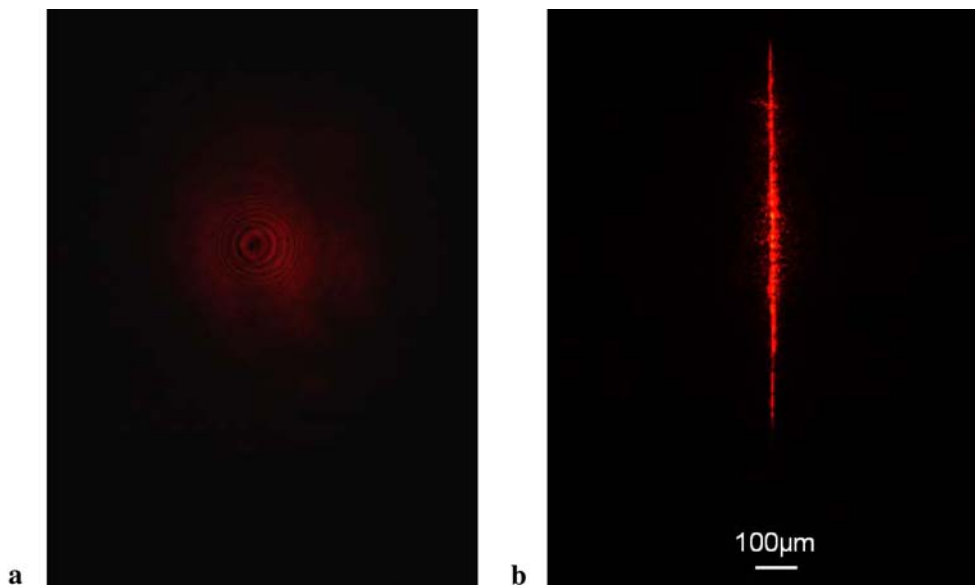


FIGURE 2 CCD camera images of (a) He-Ne laser beam; and (b) He-Ne laser beam focused by a microoptical cylindrical lens

ison, we show scanning electron microscopic (SEM) images of both the microcylindrical lenses with and without the final annealing step at 560 °C. It is clear in Fig. 1a that the sample without the final annealing step shows a rough surface composed of periodic ring structures. The period of the ring array is approximately 15 μm, which is consistent with our fabrication parameter. However, after the second annealing step at 560 °C, the sample surface became much smoother, as can be seen in Fig. 1b. The smooth surface is critical for optical applications of the buried structures, since otherwise the scattering caused by the surface roughness will induce significant loss and destroy the wave-front of the optical beam.

Next, we examined the focusing ability of the microoptical cylindrical lenses using a He-Ne laser. In this experiment, first, we let the He-Ne laser beam pass through a cylindrical lens. After the cylindrical lens, a 10× objective lens was used to form an enlarged image of the focal beam spot produced by the cylindrical lens onto a CCD camera (Sony XCD-710CR). As shown in Fig. 2a, when the He-Ne laser beam directly passed through the objective lens without passing through the cylindrical lens, it exhibited a Gaussian beam profile in the CCD camera image. To avoid overexposure, we used several ND filters to reduce the power of the He-Ne laser, which caused the concentric interference rings in Fig. 2a. Shown in

Fig. 2b is the CCD camera image of the He-Ne laser beam passing through both the microoptical cylindrical lens and the 10× objective lens. Clearly, the beam was focused into a thin line with an approximate line-width of 40 μm. To decide the focal spot size, we used the same optical system to take an image of a microoptical grating with a pitch of 10 μm. Comparison of the images of the microoptical grating and of the linear focal spot gives out the magnification of the imaging system.

Furthermore, we fabricated a microoptical hemispherical lens with a radius of 1 mm, as shown in Fig. 3a. The cylindrical structure below the hemispherical lens was designed to support the hemispherical lens. Both the spherical and the cylindrical structures were fabricated simultaneously in a single process. The focal beam spot produced by the upper hemispherical lens is shown in Fig. 3b. The measured focal spot size, which has a nearly symmetric beam profile, is approximately 30 μm. This result is consistent with the measured line-width of the linear focal spot in Fig. 2b.

4 Discussion and conclusion

Generally, 2D microoptical lens arrays can be fabricated on the surfaces of different materials like glasses or polymers using various microfabrication techniques. However, in many lab-on-a-chip applications, 3D microoptical lenses vertically embedded in transpar-

ent materials are desirable [7]. Because our technique allows for fabrication of the 3D microoptical components as well as the 3D microfluidic structures in one glass chip by a single process [5, 6, 8], these tiny 3D lenses can be easily integrated into a lab-on-a-chip for either focusing an optical beam into an interested area of the microfluidic channel for fluorescence detection or creating an image of the dynamic process in a microfluidic chamber. The focal spot size of these microlenses is smaller than or comparable to the typical dimensions of the microfluidic channels in most lab-on-a-chip devices. If the focusing quality can be improved, it would also be possible to use these 3D microoptical lenses for laser trapping or multi-photon fluorescence excitations.

It should be noted that the focal beam spot sizes (30 μm ~ 40 μm) reported here are significantly larger than the theoretical values. Assuming a beam size of 0.7 mm and a wavelength of 632 nm for the He-Ne laser, and a focal length of 2 mm for the microoptical hemispherical lens (using a refractive index of 1.5 for Foturan glass), the calculated focal spot size (diameter of airy disk) is only 4.25 μm. We attribute the degraded focusing performance to the surface deformation which causes deviation of the fabricated surface from the designed surface. Restricted by our experimental instrument, we cannot measure the surface profile across the whole lens surface. Our previous investigations showed that an average rough-

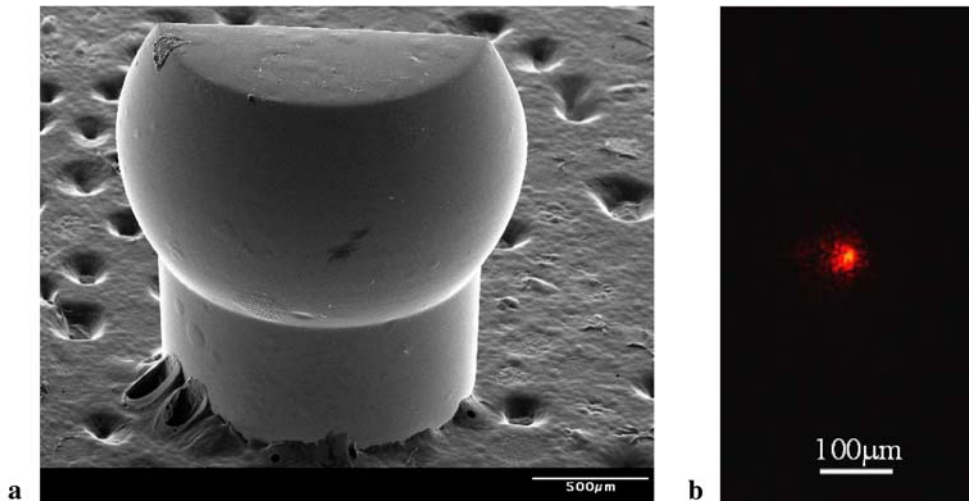


FIGURE 3 (a) SEM image of a microoptical hemispherical lens; (b) CCD camera image of a He-Ne laser beam focused by a microoptical hemispherical lens

ness of approximately 0.8 nm of a planar structure (scanning area $20\ \mu\text{m} \times 20\ \mu\text{m}$) could be achieved with the second annealing [14]. Although the measured surface roughness is low, the surface uniformity in a large area could still be imperfect due to the deformation caused by the post-annealing.

The mechanism of the surface smoothening of Foturan glass at $560\ ^\circ\text{C}$ could be understood in a way similar to the surface melting of ice [15], where a thin layer of liquid could be formed on the surface of the ice when the ambient temperature is below the melting point. The surface tension in this liquid layer can help form a smooth surface on the glass. Since the thickness of the liquid layer on the surface is dependent on the ambient temperature and thermal-physical properties of the liquid (e.g., viscosity), controlling the annealing temperature for smoothening the glass surface is critical. If the annealing temperature is too high, the thickness of the surface liquid layer would increase, then the surface tension might not be adequate to overcome other forces like gravity, hence the localized surface deformation might occur. If the annealing temperature is too low, the thickness of the liquid layer would be too small to get rid of the surface roughness. Therefore, there is a trade-off in selecting the

proper annealing temperature. In addition, the compositional uniformity of the Foturan glass is also critical for the microstructuring of Foturan glass [16]. If the silver ions are not uniformly distributed in the glass matrix, different etching rates would occur at different areas even with the same exposure conditions. Additionally, the internal stress in the glass could also induce localized deformation during the second annealing process. Therefore, the key to achieving a smooth surface of nm-scale roughness and flatness across a large area (hundreds micron to several millimeter) may depend on the material itself.

To summarize, we have demonstrated the fabrication of 3D microoptical lenses in glass using a home-integrated fs laser micromachining system. Integrating these tiny lenses with microfluidic structures is underway for producing novel lab-on-a-chip devices.

ACKNOWLEDGEMENTS We wish to thank N.K. Kondameedi, Y. Han, and R.A. Powell in the Mechanical & Aerospace Engineering Department, UMR for their help in the experiments. Support from Prof. Yinfa Ma of the Chemistry Department, UMR in chemical etching is greatly appreciated. This work was supported by the Air Force Research Laboratory under Contract No. FA8650-04-C-5704 and the National Science Foundation under Grant No. 0423233.

REFERENCES

- 1 D. Figeys, D. Pinto, *Anal. Chem.* **72**, 330A (2000)
- 2 M.A. Burns, B.N. Johnson, S.N. Brahmasandra, K. Handique, J.R. Webster, M. Krishnan, T.S. Sammarco, P.M. Man, D. Jones, D. Heldsinger, C.H. Mastrangelo, D.T. Burke, *Science* **282**, 484 (1998)
- 3 V. Lien, K. Zhao, Y. Lo, *Appl. Phys. Lett.* **87**, 194 106 (2005)
- 4 S. Balslev, A. Kristensen, *Opt. Express* **13**, 344 (2005)
- 5 Y. Cheng, K. Sugioka, K. Midorikawa, *Opt. Express* **13**, 7225 (2005)
- 6 Y. Cheng, K. Sugioka, K. Midorikawa, *Opt. Lett.* **29**, 2007 (2004)
- 7 K.W. Ho, K. Lim, B.C. Shim, J.H. Hahn, *Anal. Chem.* **77**, 5160 (2005)
- 8 M. Masuda, K. Sugioka, Y. Cheng, N. Aoki, M. Kawachi, K. Shihoyama, K. Toyoda, H. Helvajian, K. Midorikawa, *Appl. Phys. A* **76**, 857 (2003)
- 9 H. Helvajian, P.D. Fuqua, W.W. Hansen, S. Janson, *RIKEN Rev.* **32**, 57 (2001)
- 10 Y. Cheng, K. Sugioka, K. Midorikawa, M. Masuda, K. Toyoda, M. Kawachi, K. Shihoyama, *Opt. Lett.* **28**, 55 (2003)
- 11 Y. Kondo, J. Qiu, T. Mitsuyu, K. Hirao, T. Yoko, *Japan J. Appl. Phys.* **38**, L1146 (1999)
- 12 T. Hongo, K. Sugioka, H. Niino, Y. Cheng, M. Masuda, J. Miyamoto, H. Takai, K. Midorikawa, *J. Appl. Phys.* **97**, 063 517 (2005)
- 13 V.R. Bhardwaj, E. Simova, P.B. Corkum, D.M. Rayner, C. Hnatovsky, R.S. Taylor, B. Schreder, M. Kluge, J. Zimmer, *J. Appl. Phys.* **97**, 083 102 (2005)
- 14 Y. Cheng, K. Sugioka, K. Midorikawa, M. Masuda, K. Toyoda, M. Kawachi, K. Shihoyama, *Opt. Lett.* **28**, 1144 (2003)
- 15 R. Rosenberg, *Phys. Today* **58**, 50 (2005)
- 16 H. Helvajian, private discussion